A Frontal-Jet Stream Cross Section[1]

By B. W. BOVILLE, W. S. CRESWICK AND J. J. GILLIS, Central Analysis Office, Montreal, Canada

(Manuscript received December 21, 1954)

Abstract

The validity of the thermal wind relationship for determining high level winds in the vicinity of jet streams is discussed.

A cross section wind field was constructed utilizing only the thermal field for levels above 700 mb. This wind field is compared to one obtained from rawin reports.

The results indicate that a reasonable picture of the high level jet winds is obtained when vertical extrapolation is based on the thermal field analysed with respect to three-dimensional fronts.

1. Introduction

A jet-stream isotach analysis at 300 mb is carried out at the Central Analysis Office, Montreal, Canada for an area extending approximately from 30° W to 160° W and 25° N to 80° N. The density of high level wind reports does not permit an *ab initio* analysis of the asymmetric jet wind field over most of the chart. The extension of the analysis into these areas is to a large measure based on the close relationship which exists between the structures of jet streams and three-dimensional fronts. The cross sections contained in this paper were prepared as part of a training program in jet stream analysis techniques.

2. The frontal cross section

To illustrate the validity and use of the thermal wind approximation the cross section given as fig. 2 was drawn on the following basis. A line was chosen which was approximately normal to the flow and where rawin data were sufficiently dense to permit a subsequent check on the true wind structure. Upper air stations on this line were Denver, Colo., Dodge City, Kan., Topeka, Kan., Columbia, Mo., Rantoul, Ill., Dayton, Ohio, and Pittsburgh, Pa. The analysis was carried out utilizing complete tephigram plots but wind data were limited to the levels surface to 700 mb.

The tephigrams (fig. 1) show three air masses (*mT*, *mP* and *mA*) and two fronts with the top and base of each hyperbaroclinic zone being well defined. The major high level thermal contrast is between Rantoul (RAN) and Dayton (FFO) and a jet core is to be expected in the 300—250 mb layer where the thermal gradient becomes zero and then reverses.

The only structure not precisely shown by the tephigrams was for the 400—200 mb layer between Rantoul and Dayton. Inspection of neighbouring tephigrams showed a well defined Polar front to levels above 400 mb so that the extension of the frontal surface to the tropopause was valid. No conclusive evidence was available as to whether the tropopause sloped steeply or was broken in that area. The continuous structure was drawn as an adequate portrayal of the thermal gradients.

The thermal winds were calculated from the isotherms at many points using a scale based on the equation

$$\frac{\partial V_H}{\partial Z} = \frac{g}{fT}\frac{\partial T}{\partial n}$$

[1] Published by permission of the Controller, Meteorological Division, Department of Transport, Canada.

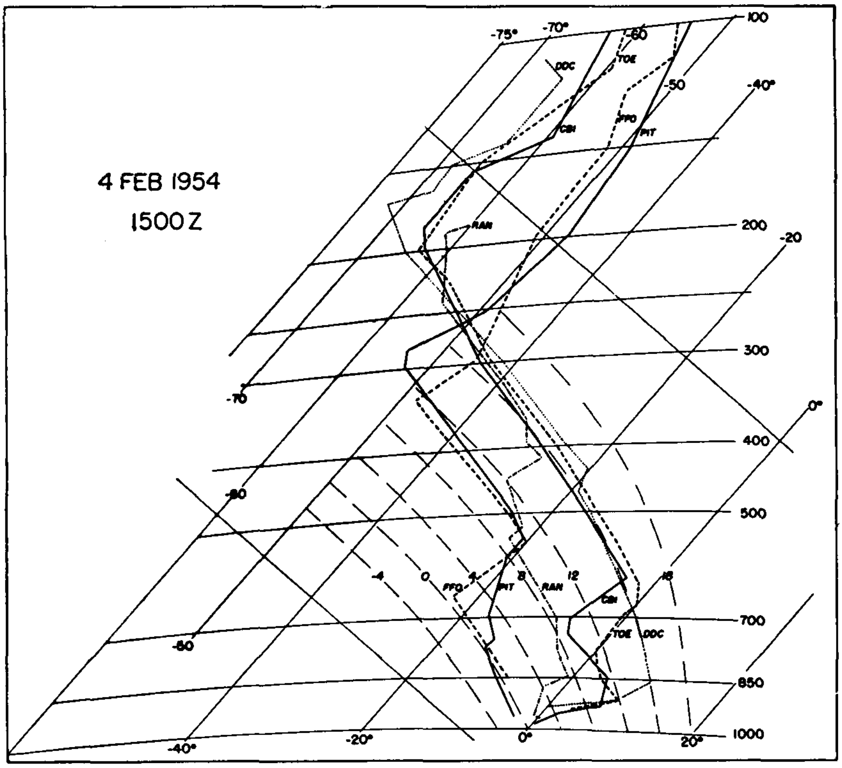

Fig. 1. Tephigrams (dry bulb curves).

Vertical addition from the observed 700 mb winds provided a dense network of calculated winds as a basis for the 20 knot isotachs.

3. Comparison of calculated and observed winds

The observed winds for all levels were plotted on a cross section on which the tropopause and fronts had been entered. The observed wind field was then drawn as shown in fig. 3. There were sufficient winds for an objective analysis except for the layer above 200 mb over Rantoul.

Comparison of the two wind fields reveals a striking similarity indicating the validity of using the thermal-wind relationship even up to levels as high as 100 mb. In general the wind increase through the frontal zones appears to be spread through a deeper layer than the calculation in fig. 2 would indicate. This may be partly real and partly due to the averaging process used in obtaining the observed winds for specific levels. The only significant discrepancy is found in the 400—200 mb layer over Topeka extending to about 250 mb over Columbia. The observed winds are 20—40 knots greater than the calculated winds.

The calculated winds are based on the assumption that addition of the geostrophic-thermal wind to the observed 700 mb wind yields a correct high-level wind. This is, in effect, assuming that any ageostrophic components have the same magnitudes from 700 mb up. For pressure systems with vertical axes this is a reasonable assumption in percentage terms but not in absolute terms due to the higher wind speeds at upper levels (e.g. the curvature term contains the square of the wind speed). Since the wind excess over Topeka is in the same direction as the geostrophic wind its explanation should be sought in terms of anticyclonic curvature.

4. Application of the equation of horizontal motion

From the equation of horizontal motion, after PRIESTLEY (1948), it may be shown that:

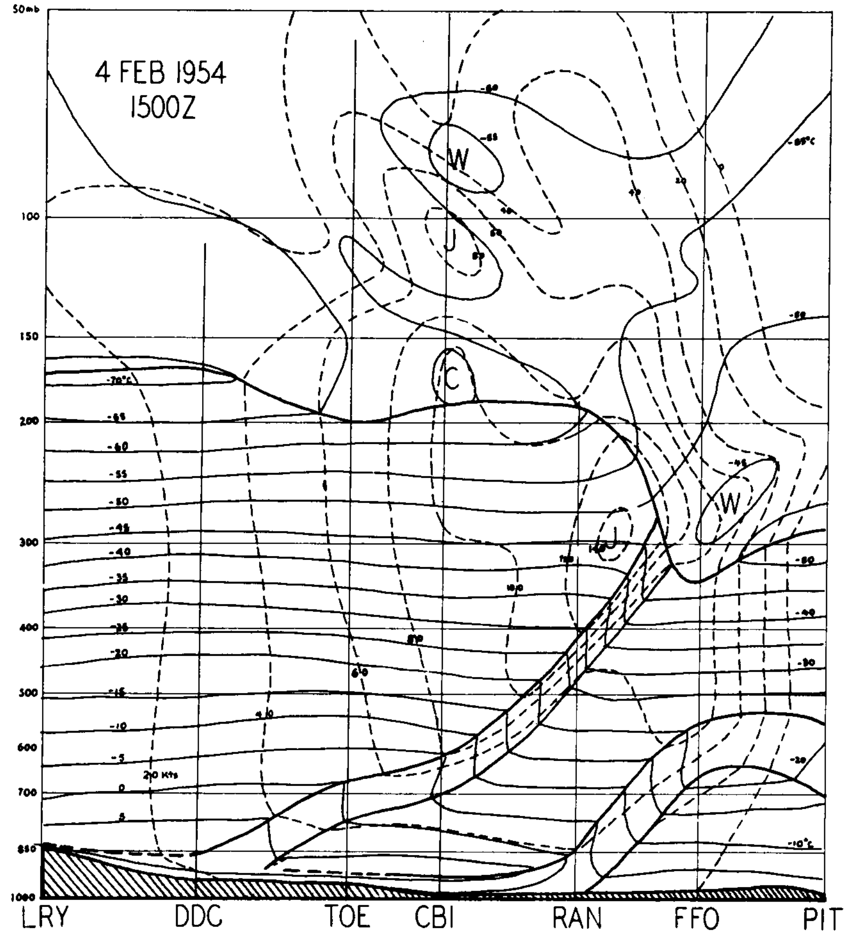

Fig. 2. Vertical Cross Section.
Solid heavy lines—fronts, tropopause.
Solid thin lines—isotherms °C.
Dashed thin lines—isotachs (computed).

$$\vec{V}_H = \vec{V}_g - \frac{K_{Ht}}{f} V_{Ht}^{2}\vec{t} + \frac{\dot{V}_H}{f}\vec{n} + \frac{w}{f}\vec{k} \times \frac{\partial \vec{V}_H}{\partial Z} + \vec{j} \cot \varphi w$$

where $\vec{t}$, $\vec{n}$, $\vec{k}$, $\vec{j}$ are respectively, tangential, normal, vertical and northward unit vectors in relative coordinate systems and the other symbols have their usual meaning.

To show an indication of the relative magnitudes of the geostrophic departures the individual terms of this equation were considered.

4.1. The curvature term $\frac{K_{Ht}}{f} V_H^{2}\vec{t}$

Inspection of the 300 mb contours in the Topeka area indicates a straight or slightly cyclonically curved field which would appear to negate a curvature explanation for the wind excess. However, examination of the actual wind reports reveals considerable cross contour flow and there are sufficient reports to permit an independent streamline analysis for the area. The streamlines, as in fig. 4, do show anticyclonic curvature over a considerable portion of the cross section area. K_H, the curvature of the trajectory, may be related to K_s, the

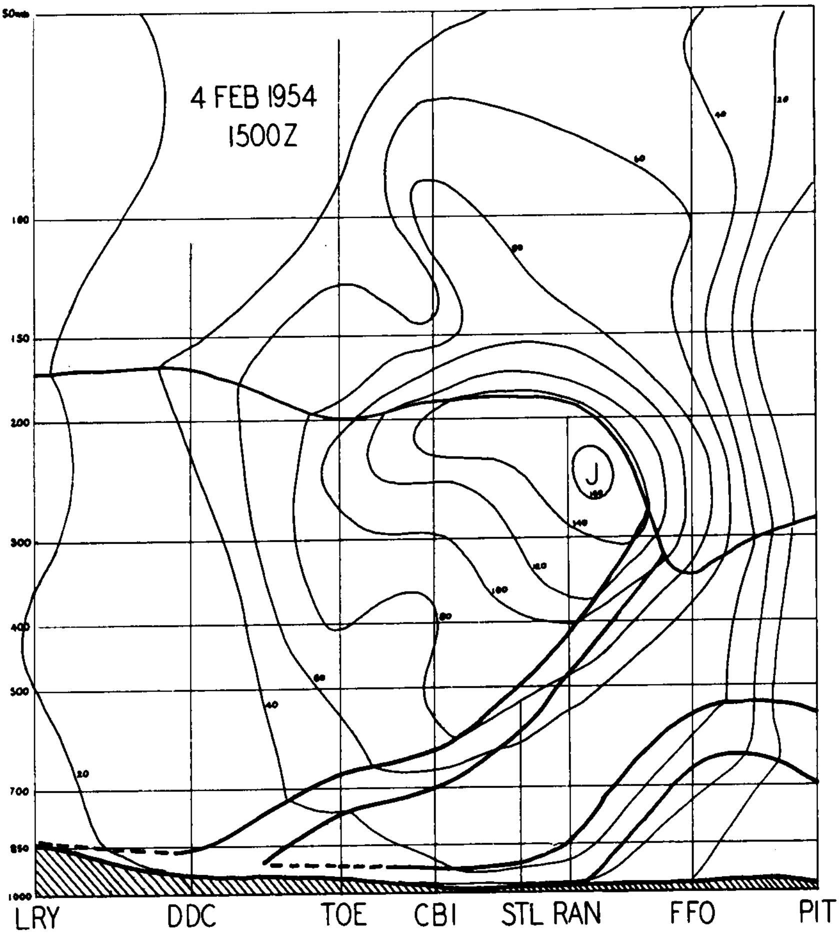

Fig. 3. Vertical Cross Section.
Solid heavy lines—fronts, tropopause.
Solid thin lines—isotachs (observed).

curvature of the streamline, through the equation

$$K_{Ht} V_H = K_s (V_H - C \cos \varphi)$$

where $C \cos \varphi$ is the component of motion of the pressure system in the direction of V_H.

Measurements on fig. 4 give anticyclonic streamline curvature of about 1/600 nm east of Dodge City decreasing to zero near Columbia thence the cross section line remains near the inflexion point of the streamlines to the jet axis. Measurements from surface and upper level charts show a short wave system moving through the area, in the direction of the flow, at about 30 knots.

Inspection of fig. 2 and 4 reveals the following: In the vicinity of Dodge City the motion ($C \cos \varphi$) approximates the wind speed (V_H) and also since V_H itself is small the curvature term will be small. Near Topeka there is still considerable curvature combined with strong winds and a strong wind increase above 700 mb and the curvature term may be significant. From St. Louis to Rantoul $K_s = 0$ thus the curvature term will be zero. From the foregoing equations the K_s at Topeka required to give the wind excess of V_H (fig. 3) over V_g (fig. 2) at 300 mb can be computed as follows

	V_H	V_g	$V_H - V_g$	K_t	K_s
TOE	94 kts	68	26	1/1,000 nm	1/680 nm

(300 mb)

The measured K_s in the vicinity of Topeka

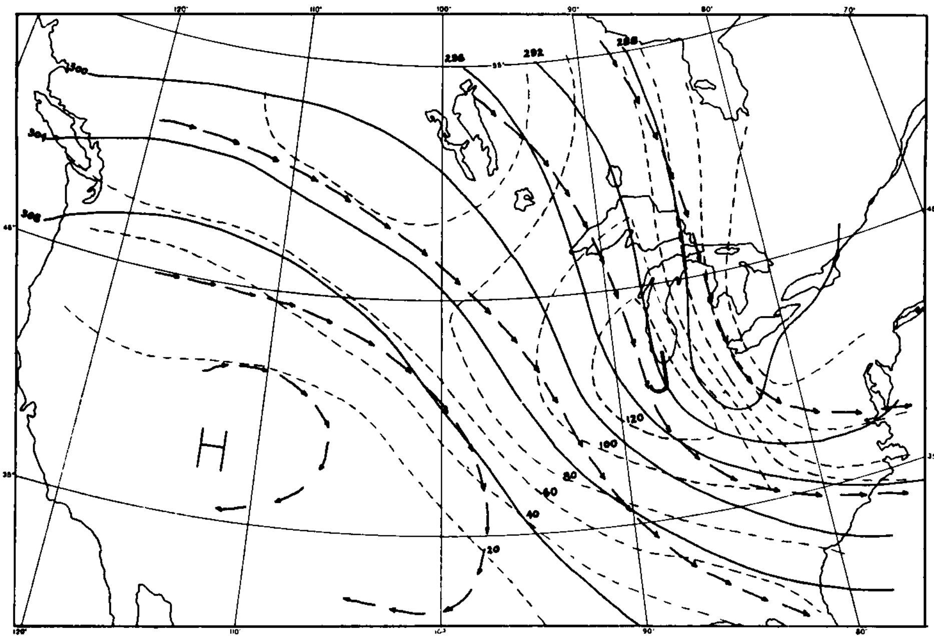

Fig. 4. 300 mb Chart (4 Feb. 1954—1500Z).
—— Contours.
→ → Streamlines.
---- Isotachs (knots).

is of the order of 1/700 nm and thus the wind excess can be adequately explained in terms of streamline curvature.

4.2. The acceleration term $\frac{\dot{V}_H}{f}\vec{\mathbf{n}}$

The action of the acceleration term where n is normal to the trajectory towards lower pressure is strikingly demonstrated in the Bismarck to Memphis area of fig. 4. The streamlines are seen to cross the contours towards lower heights where V_H is increasing along the streamline, become parallel as the maximum is reached and cross towards higher heights where the wind decreases. The following computations were made for Des Moines using:

$$\dot{V}_H = \frac{\partial V_H}{\partial t} + \vec{\mathbf{V}}_H \cdot \frac{\partial \vec{\mathbf{V}}_H}{\partial s}$$

$\frac{\partial V_H}{\partial t} = -20$ kts/6 hours (from successive rawins)

$V_H = 100$ kts, $\frac{\partial V_H}{\partial S} = 20$ kts/200 nm

$$\frac{\dot{V}_H}{f} = \frac{\frac{-20}{6} + 100 \times \frac{20}{200}}{f(\text{hour}^{-1})} = 23 \text{ kts.}$$

This gives an angle between V_H and V_g of 13 degrees.

4.3. The vertical motion term $\left(\frac{w}{f}\vec{\mathbf{k}} \times \frac{\partial \vec{\mathbf{V}}_H}{\partial Z}\right)$

This term will, in general, be of significance when both the vertical motion and vertical shear (of V_H) are relatively large such as in the vicinity of fronts and jet streams.

The term arises from a consideration of the effect of vertical motion in the total differential dV_H/dt

$$\text{i.e. } \frac{dV_H}{dt} = \frac{\partial V_H}{\partial t} + \vec{\mathbf{V}}_H \cdot \frac{\partial \vec{\mathbf{V}}_H}{\partial s} + \vec{\mathbf{w}} \cdot \frac{\partial \vec{\mathbf{V}}_H}{\partial t}$$

Thus it represents an acceleration due to ascent or descent where V_H varies vertically in the same manner as $\vec{\mathbf{V}}_H \cdot \frac{\partial \vec{\mathbf{V}}_H}{\partial s}$ represents motion across the horizontal isotach field.

A qualitative application of this term can be obtained by using the thermal wind relationship as a first approximation for $\frac{\partial \vec{\mathbf{V}}_H}{\partial Z}$. The term can then be assessed in terms of horizontal temperature gradients. Thus ascent gives a horizontal component of motion from warm to cold air; descent gives a horizontal component of motion from cold to warm air.

In the vicinity of jet streams some further assumptions can be made regarding the distribution of V_H. The vertical shears are usually parallel to the wind (wind direction changes little with height) and thus the term can be expressed as a component normal to the streamlines,

$$\text{i. e.}\ \frac{w}{f}\vec{\mathbf{k}}\times\frac{\partial V_H}{\partial Z}\vec{\mathbf{t}}=\frac{w}{f}\frac{\partial V_{H+}}{\partial Z}\vec{\mathbf{k}}\times\vec{\mathbf{t}}=\frac{w}{f}\frac{\partial V_H}{\partial Z}\vec{\mathbf{h}}$$

In this form the effect of the term is seen to be similar to that of the horizontal acceleration term (4.2).

Since the sign of the vertical shear changes across the jet core it follows that:

(a) above the jet core ascent gives a component of horizontal motion towards higher pressure and subsidence towards lower pressure.

(b) below the jet core the reverse holds.

The requirement for vertical motion in this term makes computations rather difficult. However, two have been attempted with the realization that possible errors may be large.

In the vicinity of Sault Ste. Marie (SSM) the streamlines cross the contours towards lower pressure and at the same time the wind speed decreases along the streamline. If the contour streamline pattern is right then it is clear that the vertical-motion term must be rather strong. There is a sharp tropopause at 300 mb at SSM coinciding with a reversal of vertical wind shear. Since the wind direction remains constant along the streamline from 30,000 to 35,000 feet while the wind speed drops 7 knots an evaluation will be made on this basis.

$$V_H=45\ \text{kts}\quad \frac{\partial V_H}{\partial Z}\vec{\mathbf{t}}=-7\,\text{kts}/5{,}000\ \text{ft}$$

The angle between V_H and $V_g \simeq 10$ degrees and the required cross component is 45 sin 10° = 8 kts. The expression can now be solved for w

$$w=\frac{f}{\partial V_H/\partial Z}Vn=-0.32\ kts\simeq-16\ \text{cm/sec}$$

Thus subsidence of 16 cm/sec just above 300 mb is required to account for the cross-wind component. A somewhat higher figure would be required to balance the horizontal deceleration as well.

At 300 mb over Dayton (FFO) there is appreciable increase of wind with height and judging by the low tropopause and high 300 mb temperature considerable subsidence. For w negative and $\frac{\partial V_H}{\partial Z}$ positive $\left(\frac{\partial \vec{\mathbf{V}}_H}{\partial Z}\,//\,\vec{\mathbf{V}}_H\right)$ this represents a velocity component normal to the flow towards higher pressure.

$\frac{\partial V_H}{\partial Z}=4$ kts/1,000 ft; using a w calculated on the basis of the observed temperature gradient at 300 mb upstream from Dayton and subsidence along a dry adiabat, $w = -.17$ kts ($\simeq -8.5$ cm/sec). This gives a cross component towards higher pressure = 12 kts and is equivalent to an angle between V_H and V = 7 degrees.

Since the computed values of vertical motions and cross-contour flow are of the same order as those usually quoted it appears that qualitatively at least they may be of significance. However, it should be noted that most of the computed values also fall within the range of the possible errors of the observed values.

4.4. The latitude term ($\vec{\mathbf{j}}\cos\varphi w$)

This term is usually very small and represents an easterly component for subsidence and a westerly component for ascent. The value of this term for the subsidence figure in 5.3 is $-.17 \times 1.2 = -0.2$ kts.

4.5. It thus appears that although the thermal approximation gives very good results when used to calculate the overall wind field, other terms in the velocity equation can give appreciable contributions to the total wind. The use of the thermal wind approximation will be most valid when extrapolations are done vertically within a similar pressure and wind

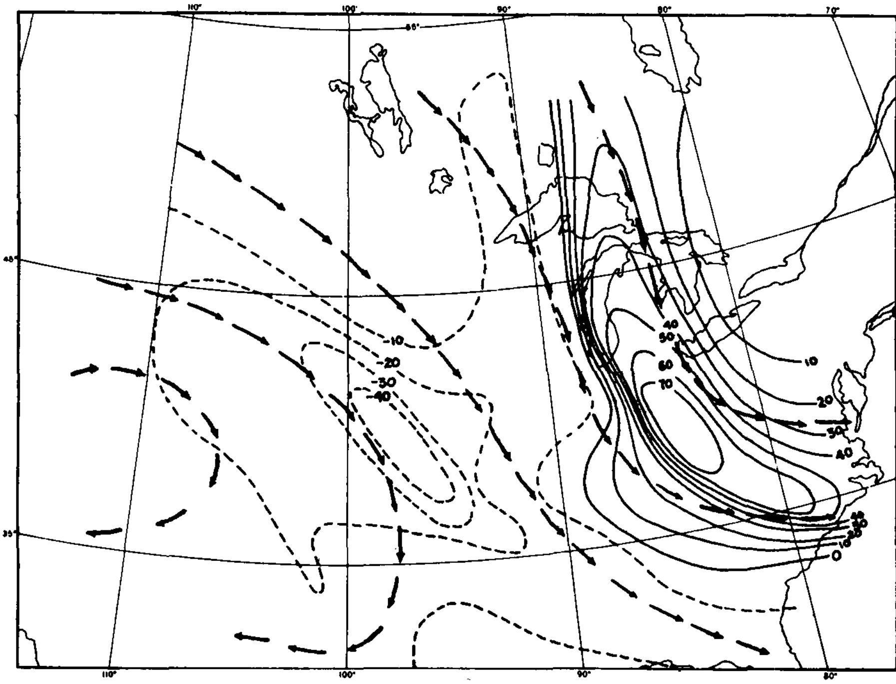

Fig. 5. 300 mb Chart (4 Feb. 1954—1500Z).
——, - - - - Isolines of relative vorticity ($\text{hour}^{-1} \times 10^{-2}$).
→ → Streamlines.

field, e.g. extrapolation to 300 mb from an observed 500 mb wind will normally have the ageostrophic components incorporated in the 500 mb wind. Absolute errors will increase in areas where there is strong curvature change or strong vertical motion.

5. The vorticity field at 300 mb

The distribution of the vertical component of relative vorticity at 300 mb is given in fig. 5. This field was computed from the data given by fig. 4 using the expression for relative vorticity (e.g. HOLMBOE, 1945).

$$\zeta = \frac{V_H}{R_s} - \frac{\partial V_H}{\partial n}$$

The two terms were computed independently using units of knots and 100 nm and then added to give the total relative vorticity. The data given in fig. 5 are thus in units of $\text{hour}^{-1} \times 10^{-2}$ which is 36×10^4 times the standard vorticity unit of sec^{-1}. In terms of the units of fig. 5 the coriolis parameter (f) at 40° N is equal to 33.7.

The horizontal wind shear is so strong, in the vicinity of the jet stream at 300 mb, that this term generally predominates in the vorticity calculations. However, the curvature term is strong enough to produce cyclonic vorticity to the west of the jet axis in the vicinity of Nashville (BNA). To the west of Topeka (TOE) where it has the same sign as the shear term the two produce a small region where anticyclonic vorticity exceeds the coriolis parameter.

6. Relation of the vorticity field to surface pressure change

The surface pressure changes, in millibars, between 1230 Z and 1830 Z are given in fig. 6. Since this period overlaps the upper air time of 1500 Z the surface changes and the 300 mb vorticity field can be compared.

The relationship between the surface pressure change and the relative vorticity field has been treated by a number of writers (e.g. SUTCLIFFE, 1947; RIEHL, 1952).

From their derivations the following quali-

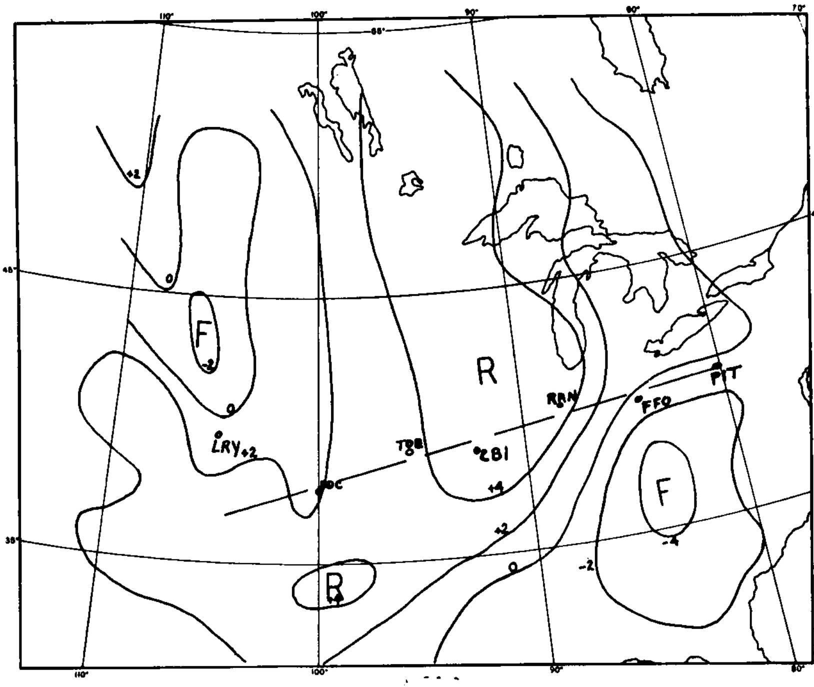

Fig. 6. Surface Pressure Change Chart.
1230Z to 1830Z 4 Fec. 1954 (whole millibars).

tative relationships, applicable to a barotropic atmosphere, can be inferred:

$$\text{sign of } \frac{dP_0}{dt} = \text{sign of } (-\text{div}_{300} V_H) = \text{sign of}$$

$(\vec{V}_H \cdot \nabla \zeta)$ subscript

Thus if the cyclonic (relative) vorticity at 300 mb decreases (or anticyclonic vorticity increases) downstream the contribution of this term is for a surface pressure fall. The opposite is also true.

From figures 5 and 6 it can be seen that there is good agreement between the surface pressure changes and the advection of vorticity. The maximum pressure falls to the southeast of Dayton (CVG)—Nashville (BNA) are just to the south of the normal axis of maximum cyclonic vorticity. The pressure rises in the St. Louis (STL)—Rantoul (RAN) area lie in a region where $(\vec{V}_H \cdot \nabla \zeta)_{300}$ is positive. Also the line of pressure rises and falls in the Casper (CPR)—Goodlands (GLD)—Oklahoma City (OKC) region is close to the line of vorticity changes associated with anticyclonic maximum.

REFERENCES

HOLMBOE, GUSTIN, and FORSYTH: *Dynamic Meteorology*, Wiley 1945.

PRIESTLEY, C. H. B., 1948: *Australian Journal of Scientific Research*, Vol. 1, pp. 41—57.

SUTCLIFFE, R. C., 1947: *Q. J. R. Met. Soc.* **73**, p. 370.

RIEHL, H., et al, 1952: *Meteorological Monograps*, Vol. 1, No. 5.